



Published in final edited form as:

Lab Chip. 2016 July 7; 16(13): 2504–2512. doi:10.1039/c6lc00081a.

Microfluidics 3D gel-island chip for single cell isolation and lineage-dependent drug responses study

Zhixiong Zhang^{#a}, Yu-Chih Chen^{#a,c}, Yu-Heng Cheng^a, Yi Luan^b, and Euisik Yoon^{*,a,b}

^aDepartment of Electrical Engineering and Computer Science, University of Michigan, 1301 Beal Avenue, Ann Arbor, MI 48109-2122

^bDepartment of Biomedical Engineering, University of Michigan, 2200 Bonisteel, Blvd. Ann Arbor, MI 48109-2099, USA

^cUniversity of Michigan Comprehensive Cancer Center, 1500 E. Medical Center Drive, Ann Arbor, MI 48109, USA

These authors contributed equally to this work.

Abstract

3D cell culture in the extracellular matrix (ECM), which not only provides structural support to cellular constituents, but also initiates regulatory biochemical cues for a variety of important cell functions in tissue, has become more and more important in understanding cancer pathology and drug testing. Although the ECM-gel has been used in cell culture both in bulk and on-chip, previous studies focused on collective cell behavior rather than single-cell heterogeneity. To track the behavior of each individual cell, we have developed a gel-island chip, which can form thousands of islands containing single cells encapsulated by the desired ECM. Optimized by Poisson's distribution, this device can attain 34% capture efficiency of the exact number of single cells per island. A good culture media exchange rate and high cell viability can be achieved in the gel-islands. The cells in the islands can be automatically counted for high-throughput analysis. As a proof of concept, we monitored the proliferation and differentiation of single Notch+ (stem-like) T47D breast cancer cells. The 3D collagen gel environment was found to be favorable for the stem-like phenotype through better self-renewal and de-differentiation (Notch- to Notch+ transition). More interestingly, we found that the Notch- de-differentiated cells were more resistant to doxorubicin and cisplatin than the Notch+ cells. Combining the 3D ECM culture and single cell resolution, the presented platform can automatically analyze the individual cell behaviors of hundreds of cells using a small amount of drug and reagents.

Keywords

3D cell culture; extracellular matrix; ECM; collagen; single cell; cell heterogeneity; differentiation; drug screening

*Corresponding author, Euisik Yoon, 1301 Beal Avenue, Ann Arbor, MI 48109-2122, USA, Tel: 734-615-4469; esyoon@umich.edu. Zhixiong Zhang, 1301 Beal Avenue, Ann Arbor, MI 48109-2122, USA, Tel: 734-353-0400; zhangzx@umich.edu.

Competing financial interests

The authors declare no competing financial interests.

Introduction

In vitro cell culture has been widely used in cell behavior studies for more than 100 years. However, it is not until the 80s that people started to highlight the importance of 3D cell culture, especially for understanding the roles of the extracellular matrix (ECM) in tissue physiology and cancer pathology [1]. To bridge the different drug responses between conventional 2D cell culture and in vivo experiments, more and more cancer researchers are performing experiments in the more realistic 3D culture environment [2-3]. Compared to the 2D culture, which grows cells on artificial rigid polystyrene (Young's modulus: 3 GPa) or glass (Young's modulus: 50-90 GPa), the 3D culture grows cells in the elastic ECM (Young's modulus: 50-5000 Pa, depending on the tissue) environment and can better mimic the in vivo environment [4-7]. In addition to their mechanical property, cells are known to sense the biochemical signals from the surrounding ECM using various signal transduction cascades via receptors on the cell membrane [8]. Therefore, it is important to apply 3D ECM culture in microfluidics for re-capitulating the tumor microenvironment.

Due to the genomic and epi-genomic instability of tumors, cancer cells are notorious for their heterogeneity. Among the various sub-populations, cancer stem-like cells (CSCs), which play critical roles in cancer metastasis, therapeutic resistance, and relapse, are important clinical targets [9-12]. As stem-like cells, CSCs are capable of either self-renewal (symmetric division) to generate CSCs or differentiation (asymmetric division) to make differentiated cancer cells [13]. Considerable evidence suggests that the symmetric division of CSCs is critical for the progression of tumors, whereas skewing toward asymmetric division can lead to tumor suppression [14-15]. Although it is believed that the 3D culture environment is favorable for stem-like phenotypes, it is not clear whether this is caused by (1) reduced asymmetric division, (2) increased symmetric division, or (3) better survival of stem-like cells [16-17]. In addition, CSCs are typically more resistant to chemotherapies; however, it is not clear whether self-renewing CSCs have stronger resistance compared to differentiating CSCs [18-19]. Using the conventional dish-based approach, only the final cell number and gene expression (or Live/Dead) can be counted by fluorescence-activated cell sorting (FACS). The averaged end-point results provide little insight into the cellular heterogeneity of CSCs and not the process of how the population is skewed. To decipher the changes of CSC populations in different conditions and treatments, there is a need for single cell analysis to monitor the fate of each individual cell.

Due to the benefits of small sample volumes, precise fluid control, and high-throughput scaling, microfluidic technology has emerged as a state-of-the-art approach for single cell analyses [20-24]. There are a number of previous reports on microfluidic platforms for 3D cell culture, but many of them use a suspension culture with hydrogel, which cannot emulate the cell-ECM interactions in vivo [25-27]. To incorporate 3D ECM in microfluidics, some researchers control the hydrogel matrix using laminar flow [28], surface tension (achieved using micropillars) [29], and physical confinements [30-31], but these cannot achieve precise spatial control for performing a single cell assay. Hydrogel droplet formation [32-33] and 3D bioprinting [34] encapsulating single cells have merits in high-throughput and precise micro-environment control. However, only a limited number of bio-materials can be used for these technologies, thus making it difficult to study a wide range of different ECMs,

which have distinct biochemical properties. In addition, the shear force induced by inkjet printing can compromise the cell viability. Although filling a hydrogel with cells in microwells can be one simple alternative [35], exposed microwells can easily suffer from media evaporation, which increases osmolality and thus affect cell viability. Moreover, cells will be inevitably washed away when exchanging the media in microwells. To reliably culture single cells in a 3D hydrogel for cellular heterogeneity study, we developed a gel-island chip, which attains (1) reliable single cell encapsulation in a hydrogel-based 3D culture, (2) high-throughput assay of hundreds of single cells, (3) automatic single cell monitoring for cellular heterogeneity characterization, and (4) efficient use of ECMs and reagents.

Experimental

Device Fabrication

The gel-island chip is composed of one layer of PDMS (polydimethylsiloxane), which was fabricated on a silicon substrate via standard soft lithography and a glass slide. Each microfluidic chip contains 1500 chambers with a 2.25 nL ($150\ \mu\text{m} \times 150\ \mu\text{m} \times 100\ \mu\text{m}$) volume capacity. The main channel was designed to be 200 μm in width to ensure sufficient culture media or drug supply near the entrance of each chamber. One mask was used to fabricate the 100 μm thick SU8 (Microchem) for the microfluidic channel. 40 grams of PDMS was cured at 100°C for 1 day and then peeled off from the master. After punching the inlet and outlet using a 0.6 mm diameter biopsy punch, the PDMS layer activated by oxygen plasma treatment (80 Watts, 60 seconds) was bonded to the glass slide. The bonded device was placed on a hot plate at 80°C for 5 minutes to enhance the bonding strength.

Lentiviral transduction

T47D breast cancer cells were transduced with pGreenFire1-Notch lentiviral (System Biosciences, Mountain View, CA) particles using standard protocols. Lentiviruses were prepared using 3rd generation helper plasmids to generate VSVG pseudotyped particles (roughly 1×10^7 units/mL) by the University of Michigan Vector Core. 500,000 T47D breast cancer cells/well ($50,000/\text{cm}^2$) were plated in a 6-well plate, and transduced the following day at an MOI of 10 for 24 hr. Transduction efficiency was ~90% at 1 week post transduction based on FACS analysis of eGFP from cells transduced with pGreenFire-CMV. GFP+ cells were collected by flow cytometry sorting using a MoFloAstrios cytometer to insure all cells contained the lentiviral vector. Following cell culture, GFP- cells were generated from GFP+ cells after reaching equilibrium.

Cell culture

Several breast cancer cell lines, such as MDA-MB-231 and T47D, were cultured both in bulk and in the gel-island chip. MDA-MB-231 cells were obtained from Dr. Gary Luker's Lab (University of Michigan, MI, USA). T47D cells were obtained from Dr. Max Wicha's Lab (University of Michigan, MI, USA). MDA-MB-231 cells were cultured in DMEM (Gibco 11965) with 10% FBS (Gibco 10082) and 1% penicillin/streptomycin (Gibco 15070). T47D cells were cultured in RPMI (Gibco 11875) with 10% FBS (Gibco 10082)

and 1% penicillin/streptomycin (Gibco 15140). All cells were cultured in polystyrene culture dishes and passaged when they reached over 80% confluency in the dish.

Collagen gel preparation

To prepare a collagen gel solution, the final concentration and final volume of the collagen gel solution were first determined. Then, the required volume of rat tail collagen type I (3.38 mg/mL, Corning, 354236) was calculated to reach the final collagen concentration. 10% 10X DMEM, low glucose (Sigma-Aldrich, D2429) and 10% FBS (Gibco 10082) was also added to supply nutrient once gelation began. Depending on the final cell concentration in the gel, this concentration was multiplied with a factor of 5 to calculate the required cell concentration. The pH of the final mixture was adjusted to pH = 7.4 by adding sodium hydroxide (NaOH), (Sigma Aldrich, 415413). The contents in the tube were mixed thoroughly by pipetting up and down to avoid local pH variance or cell aggregates. DMEM HEPES (Life Technologies, 11300-032) was used to prepare cell suspensions, which provided supplemental buffering to the gel mixture at pH 7.2 through 7.6 and minimize the batch to batch pH variance. It is desirable to place all the solutions and tubes in a refrigerator half an hour prior to the experiment to avoid partial collagen gelation during collagen gel solution preparation.

Cell loading and single cell monitoring

Before cell loading, the chip was exposed to UV radiation to ensure sterilized conditions. For small sample loading, the prepared cell-laden collagen gel solution was pipetted into the 3 inlets on the chip at the small volume of 20 μ L each. Negative pressure generated by a Pasteur pipette bulb (~1000 Pa) was applied at all 3 outlets so that gel solution could fill the main channels. Vacuum (~0.1 atm) was applied to the inlet of vacuum channel for 100 seconds until all the culture chambers were filled with collagen gel solution. Then, air was pumped into the 3 gel-loading inlets to clear out the gel solution remaining in the main channels. The entire process was performed on ice to prevent pre-mature collagen gelation. The device was then placed in a cell culture incubator (37°C, 5% CO₂) for 30 minutes until full gelation. Then, cell culture media was added to all inlets. For cells cultured on-chip, culture media was exchange every day by disposing of all the liquid in both inlets and outlets, then placing 100 μ L new culture media in the inlets. To monitor the Notch activity, the reporter cells were imaged using a fluorescent microscope. The fluorescent intensity ratio of 48 hours and 6 hours after cell loading for the same cells were calculated as the Notch activity changes.

Image acquisition

The microfluidic chips were imaged using an inverted microscope (Nikon). Bright-field and fluorescent images were taken with a 10 \times objective and a charge-coupled device (CCD) camera (Coolsnap HQ2, Photometrics). FITC and TRITC filter sets were used for the fluorescent imaging. The microfluidic cell chamber array was scanned with a motorized stage (ProScan II, Prior Scientific). Before each scanning, the stage was leveled to ensure the image remained in focus throughout the entire imaging area. The fluorescent intensity of each cell was quantified using the Nikon Research Basics software. To cancel the

background noise and substrate absorption, the background fluorescent intensity was subtracted from the intensity of the cells.

The categorization of cancer cell states

Based on the GFP fluorescent intensity, cells were identified as Notch+ cells and Notch– cells (Fig. S1). All the viable cells were classified into 6 cell states after culture in collagen islands for 48 hours: (1) Notch+ symmetric division, defined as one Notch+ cell divided into two Notch+ cells. (2) Notch+ asymmetric division, defined as one Notch+ cell divided into one Notch+ cell and one Notch– cell. (3) Notch+ quiescent, defined as one Notch+ cell remaining as one Notch+ cell. (4) Notch– de-differentiation, defined as one Notch– cell transition to one Notch+ cell. (5) Notch– symmetric division, defined as one Notch– cell divided into two Notch– cells. (6) Notch– cell quiescent, defined as one Notch– cell remaining as one Notch+ cell in 48 hours.

Anticancer drug susceptibility test

For the demonstration of anticancer drug susceptibility testing, T47D Notch+ cells were loaded with collagen gel at a concentration of 2 mg/mL and cultured in gel-islands for 48 hours, as described above. Then, cells were treated with 0.3 μ M Doxorubicin (Cayman Chemical 15007) and 50 μ M Cisplatin (Cayman Chemical 13119) for 72 hours. The concentration of each drug was chosen based on a drug IC₅₀ experiment at the bulk level (Fig. S2). The drug solution was exchanged every 24 hours by disposing of all the liquid in both inlets and outlets, then 100 μ L new drug solution was put in the inlets. To determine the cell viability after drug treatment, cells were stained using the Live/Dead Viability/Cytotoxicity Kit for mammalian cells (Life Technologies, L-3224) and were put in an incubator (37°C, 5% CO₂) for 30 minutes, followed by fluorescence microscopy imaging. The fluorescence of Notch+ reporter cells due to GFP were negligible because it is an order of magnitude weaker than the fluorescence due to the Live/Dead staining, as shown in Fig. S3.

Automatic Cell Counting Program

The number of live and dead cells was counted automatically using a Matlab program developed by our lab. For each Live/Dead staining fluorescence microscopy image, there were three overlaid channels: brightfield, FITC, and TRIC. This program obtained the fluorescent intensity value of each pixel on the FITC channel and TRIC channel. Each pixel had a value ranging from 0 to 255 to indicate its brightness. The pixels with values greater than the pre-defined threshold were treated as “bright pixels” by the program. Any block containing over 5×5 “bright pixels” was counted as one valid cell, so that any noise, cell debris, and device defects were not included because of their small size or low fluorescent intensity. In this way, the program counted the number of live cells and dead cells, and marked them with rectangles of different colors for further analysis. The entire cell counting process takes less than 2 minutes to give results. The detailed work flow and algorithm is available in the Supplementary Note.

Data analysis and processing

The chambers that captured multiple cells were not included for analysis. The error bars are the standard deviation calculated using the Excel STDEV function. The statistical significances are determined by either the unpaired nonparametric U test or Excel student T-test, using two-tail distribution and two-sample unequal variance. The significance level of $p < 0.05$ was used to consider statistical significance. * Refers to $P < 0.05$, ** refers to $P < 0.01$, and *** refers to $P < 0.001$. Results are presented as mean \pm SD.

Results and Discussion

Design of gel-island chip

The microfluidics gel-island chip comprises 1500 individual culture chambers ($150 \mu\text{m} \times 150 \mu\text{m}$, and $100 \mu\text{m}$ in height) (Fig. 1 (a)). All the culture chambers are aligned in series and connected to a main microfluidics perfusion channel ($200 \mu\text{m}$ wide) by a narrow channel of $150 \mu\text{m}$ length and $40 \mu\text{m}$ width. A separate channel was designed in parallel with the main channel for applying vacuum, with the separation of a $50 \mu\text{m}$ -thick PDMS sidewall between the culture chambers and vacuum channel (Fig. 1 (b)). The entire microfluidics chip is divided into 3 subunits with 500 culture chambers in each subunit. These three subunits share a joint vacuum channel, so that the loading process for the entire chip can be performed simultaneously.

Single cell loading

To study single cell behavior in the 3D ECM microenvironment, which recapitulates the in vivo environment, we developed a loading scheme to form isolated collagen islands while enabling perfusion media exchange. Due to the surface tension effect, initially the main channel of the device is completely filled with fluids, leaving the air trapped inside the chambers (Fig. 2 (a)). Then, vacuum is applied to the vacuum channel next to the chambers (Fig. 2 (b)). Due to the high gas-permeability of the polydimethylsiloxane (PDMS) sidewall, air in the chambers can diffuse through PDMS into the vacuum channel gradually and drive the gel solution into the chamber. After applying vacuum for 100 seconds, the air in the chambers is completely replaced by gel solution and single cells are captured (Fig. 2 (c)). The flow resistance from the main channel to the chamber is designed to be two orders of magnitude higher than the flow resistance in the main channel. According to the Hagen-Poiseuille equation, when pumping air into the main channel, the gel solution in the main channels can be purged, while the collagen solution in the culture chambers remains (Fig. 2 (d)). Thus, isolated collagen gel islands are formed and the cell culture media can be exchanged through the main channel for long-term cell culture. Because the distribution of cells per chamber should follow a Poisson distribution, the maximized number of single-cell islands can be achieved when loading the same cell number as the total number of the chambers. Using the optimized loading density, 34% of the 1500 chambers are loaded with single cells (Fig. 2 (e, f)).

Long term cell culture capability

Because the collagen gel in the main channel was evacuated by air flow, we were able to load culture media into main channel and supply nutrient to cells in the chambers via diffusion. To characterize the diffusion rate of nutrient molecules, we created collagen islands using the method described in the previous section and then flowed dextran conjugated fluorescein (MW = 40k) in the main channel to mimic large protein molecules diffusing into the culture chambers (Fig. 3 (a)). By comparing the fluorescent intensity between the culture chambers and main channel, we verified that it takes less than 2 hours for the fluorescein concentration in the chambers to reach 80% of that in the main channel and around 4 hours to reach 90% (Fig. 3 (b)). In addition, we demonstrated that the fluorescent intensity difference between chambers upstream and downstream was less than 10% (Fig. 3 (c)), thus indicating uniform media supply throughout the device. To make sure that the location of the encapsulated cells does not lead to large variance in mass transfer, we also verified conformal biomolecule distribution inside the culture chambers (Fig. S4). The diffusion experiments suggest good media exchange capability for the cell culture. To further demonstrate the long-term cell culture capability of the reported microfluidics platform, we loaded MDA-MB-231 and T47D (breast cancer) cells into the island chip and cultured for 7 days. As shown in Fig. 3 (d), single cell derived colonies were formed in the culture chambers. The size of the on-chip colony was comparable with the bulk collagen gel culture control (Fig. S5). Using the isolated gel-islands, we were able to track individual single cell proliferation and differentiation behaviors in the 3D environment, which provide insights about cellular heterogeneity.

Cancer cell differentiation study

Using the Notch reporter system [35], the Notch activity of each individual cell was determined by its GFP expression (fluorescent brightness). To study cell proliferation and differentiation behaviors in single cell resolution, T47D cells were loaded with collagen gel at a concentration of 2 mg/mL or regular culture media (2D control) into different devices (Fig. 4 (a)). The cells loaded with collagen gel solution were cultured in the gel-island, whereas the ones loaded with media were in the 2D culture environment. After 2 days culture, although the 2D control group had a higher percentage of proliferating cells compared to the 3D environment, more Notch⁺ cells differentiated to Notch⁻ cells in the 2D environment when normalizing the total number of proliferation events (Fig. 4 (b)). In addition to the Notch⁺ cells, when characterizing the cell fate for the Notch⁻ population, we observed significantly more Notch⁻ to Notch⁺ transition cases in the 3D collagen condition than in the 2D condition (Fig. 4 (c)). Using conventional approaches, researchers cannot identify the process of skewing of the population. With the aid of the presented platform, we found that the skewing toward stem-like morphology was caused by both maintaining self-renewal potentials and de-differentiation (Notch⁻ to Notch⁺ transition). In addition to the binary separation of Notch⁺ and Notch⁻ cells, we tracked the Notch expression of each individual cell by its GFP intensity. The GFP fluorescent intensity of each individual cell was measured 6 hours and 48 hours after cell loading (Fig. S6). As shown in Fig. 4 (d), the Notch expression of cells was elevated in the 3D culture environment compared to the 2D culture. This data also support that 3D collagen condition enhances the expression of the Notch signaling pathways.

Cancer drug susceptibility test

Conventionally, people use 96-well or 384-well plates for drug screening and the results are measured by MTT-based colorimetric analysis or Live/Dead cell counting using flow cytometry. Although they have been used for decades and still prevail, these conventional assays provide limited insight about cellular heterogeneity. Moreover, despite the fact that CSC can be sorted based on the markers, the differentiation and state transition can happen before or during the drug treatment. More importantly, it is almost impossible to distinguish CSC derived from self-renewal or de-differentiation using dish based approaches. To precisely correlate the cell states and drug efficacy, the states of each single cell should be tracked before and after drug treatment. Herein, we categorize cells into 6 different states: symmetrically divided Notch+ cell, asymmetrically divided Notch+ cell, quiescent Notch+ cell, de-differentiated Notch- cell, symmetrically divided Notch- cell, and Notch- quiescent cell. (Fig. S7). Using the gel-island chip, the drug (doxorubicin, cisplatin) efficacy of each type of cell state was characterized (Fig. 5 (a)).

First, using the single cell monitoring capability of the gel-island chip, we noticed that the Notch+ cells were less sensitive to the chemo-drug than Notch- cells (Fig. 5 (b)). This observation matches well with the expectation that Notch pathways correlate with cell stemness and drug resistance [37], [38]. Second, among the proliferating cells, symmetrically divided Notch+ cells were found to be more resistant than asymmetrically divided cells (Fig. 5 (c)). Again, this difference can be explained by the higher stemness of the self-renewing cells than that of the differentiating cells. More interestingly, Notch- de-differentiated cells, which underwent the Notch- to Notch+ transition, showed significantly higher drug resistance than all the other cell states, which indicates that the de-differentiating cells can be a major contributor of drug resistance. A similar drug response pattern was observed in the two drugs we tested. This result suggests that the drug response of cancer cells is not only determined by the cell status at a single static time point but also the process of cell proliferation, differentiation, and de-differentiation. Therefore, it is importance to use single-cell tools to track individual cell behavior for understanding the heterogeneous cell responses to cancer drugs.

Conclusion

We report a gel-island chip combining single cell resolution and the 3D ECM cell culture environment. By simply applying vacuum, single cells can be loaded into the islands with gel solution. Then, the gel in the main channel is evacuated by pumping air, thus forming isolated gel-islands. Using an optimized cell concentration, the single cell capture rate can reach 34% based on Poisson's distribution. Good media exchange rate into the islands, as well as upstream and downstream uniformity was demonstrated. We also showed that cells cultured in the gel islands for 7 days maintained high viability. Using this platform, we monitored the symmetric and asymmetric division of Notch+ (stem-like) T47D breast cancer cells. Compared to conventional approaches, which only allow researchers to observe the cells skewing to stem-like morphology in 3D culture without identifying the process in single cell resolution, utilizing the presented platform, we found that the skewing was caused by both the increased self-renewal of stem-like cells and the de-differentiation of Notch-

(non-stem-like) cells. In addition, we performed the drug testing of doxorubicin and cisplatin to compare the different fates of individual Notch+ and Notch- cells. As expected, Notch+ cells were more resistant than Notch- cells. Interestingly, we found that de-differentiated (Notch- to Notch+) cells were significantly more drug resistant than Notch+ cells, which demonstrates that drug efficacy can be correlated with the state change of cells. This finding suggests the importance of monitoring single cells in the 3D ECM environment, which was not previously possible using conventional approaches.

Supplementary Material

Refer to Web version on PubMed Central for supplementary material.

Acknowledgements

This study was supported in part by the Department of Defense (W81XWH-12-1-0325) and in part by the National Institute of Health (1R21CA17585701). The Lurie Nanofabrication Facility of the University of Michigan (Ann Arbor, MI) are greatly appreciated for device fabrication. The authors also thank Dr. Gary Luker's lab and Dr. Max Wicha's lab for providing cells for the experiments.

References

1. Bissell MJ, Hall HG, Parry G. J. *Theor. Biol.* 1982; 99(1):31–68. [PubMed: 6892044]
2. Baker EL, Bonnez RT, Zaman MH. *Biophys. J.* 2009; 97(4):1013–1021. [PubMed: 19686648]
3. Lee GY, Kenny PA, Lee EH, Bissell MJ. *Nat. Methods.* 2007; 4(4):259–265.
4. Jabbari E, Sarvestani SK, Daneshian L, Moeinzadeh S. *PLoS One.* 2015; 10(7):e0132377. [PubMed: 26168187]
5. Park JS, Chu JS, Tsou AD, Diop R, Tang Z, Wang A, Li S. *Biomaterials.* 2011; 32(16):3921–3930. [PubMed: 21397942]
6. Thomson, Nick; Albig, A. College of Health Sciences Presentations. 2015:1.
7. Polacheck WJ, Li R, Uzel SG, Kamm RD. *Lab Chip.* 2013; 13(12):2252–2267. [PubMed: 23649165]
8. Lu P, Weaver VM, Werb Z. *J. Cell Biol.* 2012; 196(4):395–406. [PubMed: 22351925]
9. Maitland NJ, Collins AT. *JCO.* 2008; 26(17):2862–2870.
10. Zhou J, Zhang Y. *Cell Cycle.* 2008; 7(10):1360–1370. [PubMed: 18418062]
11. Dexter DL, Leith JT. *JCO.* 1986; 4(2):244–257.
12. Geisler JP, Rose SL, Geisler HE, Miller GA, Wiemann MC. *CME J. Gynecol Oncol.* 2002; 7:25–28.
13. Morrison SJ, Kimble J. *Nature.* 2006; 441(7097):1068–1074. [PubMed: 16810241]
14. Cicalese A, Bonizzi G, Pasi CE, Faretta M, Ronzoni S, Giulini B, Briskin C, Minucci S, Di FP, Pelicci PG. *Cell.* 2009; 138(6):1083–1095. [PubMed: 19766563]
15. Gonzalez C. *Nat. Rev. Genet.* 2007; 8(6):462–472. [PubMed: 17510666]
16. Chen L, Xiao Z, Meng Y, Zhao Y, Han J, Su G, Chen B, Dai J. *Biomaterials.* 2012; 33(5):1437–1444. [PubMed: 22078807]
17. Li F, Tan H, Singh J, Yang J, Xia X, Bao J, Ma J, Zhan M, Wong ST. *BMC Syst Biol.* 2013; 7(Suppl 2):S12.
18. Liu S, Wicha MS. *J Clin Oncol.* 2010; 28(25):4006–4012. [PubMed: 20498387]
19. Vinogradov S, Wei X. *Nanomedicine.* 2012; 7(4):597–615. [PubMed: 22471722]
20. El-Ali J, Sorger PK, Jensen KF. *Nature.* 2006; 442(7101):403–411. [PubMed: 16871208]
21. Hung PJ, Lee PJ, Sabounchi P, Lin R, Lee LP. *Biotechnol. Bioeng.* 2005; 89(1):1–8. [PubMed: 15580587]

22. Balagaddé FK, You L, Hansen CL, Arnold FH, Quake SR. *Science*. 2005; 309(5731):137–140. [PubMed: 15994559]
23. Chen YC, Cheng YH, Kim HS, Ingram PN, Nor JE, Yoon E. *Lab Chip*. 2014; 14(16):2941–2947. [PubMed: 24903648]
24. Chen YC, Ingram P, Yoon E. *Analyst*. 2014; 139(24):6371–6378. [PubMed: 25118341]
25. Ungrin MD, Joshi C, Nica A, Bauwens C, Zandstra PW. *PLoS One*. 2008; 3(2):e1565. [PubMed: 18270562]
26. Chen, YC.; Ingram, P.; Lou, X.; Yoon, E. *Proceedings of the International Conference on Miniaturized Systems for Chemistry and Life Sciences (MicroTAS '12)*. Okinawa: 2012. p. 1241-1244.
27. Chen YC, Lou X, Zhang Z, Ingram P, Yoon E. *Sci. Rep.* 2015; 5:12175. [PubMed: 26153550]
28. Kunze A, Giugliano M, Valero A, Renaud P. *Biomaterials*. 2011; 32(8):2088–2098. [PubMed: 21159379]
29. Vickerman V, Blundo J, Chung S, Kamm R. *Lab Chip*. 2008; 8(9):1468–1477. [PubMed: 18818801]
30. Zervantonakis IK, Kothapalli CR, Chung S, Sudo R, Kamm RD. *Biomicrofluidics*. 2011; 5(1):13406. [PubMed: 21522496]
31. Shin Y, Han S, Jeon JS, Yamamoto K, Zervantonakis IK, Sudo R, Kamm RD, Chung S. *Nat. Protoc.* 2012; 7(7):1247–1259. [PubMed: 22678430]
32. Tumarkin E, Tzadu L, Kumacheva E. *Integr. Biol.* 2011; 3:653–662.
33. Brouzes E, Medkova M, Savenelli N, Marran D, Twardowski M, Hutchison JB, Rothberg JM, Link DR, Perrimon N, Samuels ML. *Proc Natl Acad Sci USA*. 2009; 106(34):14195–14200. [PubMed: 19617544]
34. Murphy SV, Atala A. *Nat. Biotechnol.* 2014; 32(8):773–785. [PubMed: 25093879]
35. Bernard AB, Lin CC, Anseth KS. *Tissue Eng. Part C Methods*. 2012; 18(8):583–592. [PubMed: 22320435]
36. Hassan KA, Wang L, Korkaya H, Chen G, Maillard I, Beer DG, Kalemkerian GP, Wicha MS. *Clin Cancer Res*. 2013; 19(8):1972–1980. [PubMed: 23444212]
37. Takebe N, Harris PJ, Warren RQ, Percy Ivy S. *Nat Rev Clin Oncol*. 2011; 8(2):97–106. [PubMed: 21151206]
38. Pannuti A, Foreman K, Rizzo P, Osipo C, Golde T, Osborne B, Miele L. *Clin Cancer Res*. 2010; 16(12):3141–3152. [PubMed: 20530696]

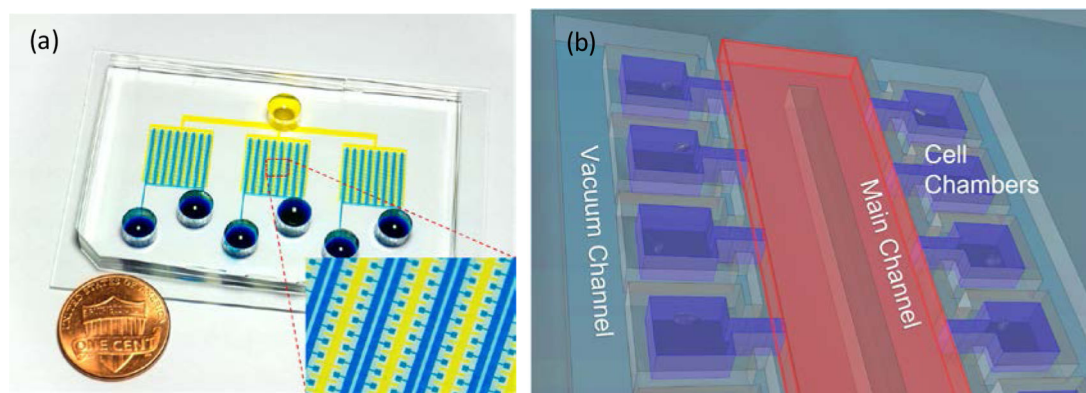


Figure. 1. Overview of the gel-island chip design (a) Image of a fabricated device. (b) Schematic of the gel-island chip.

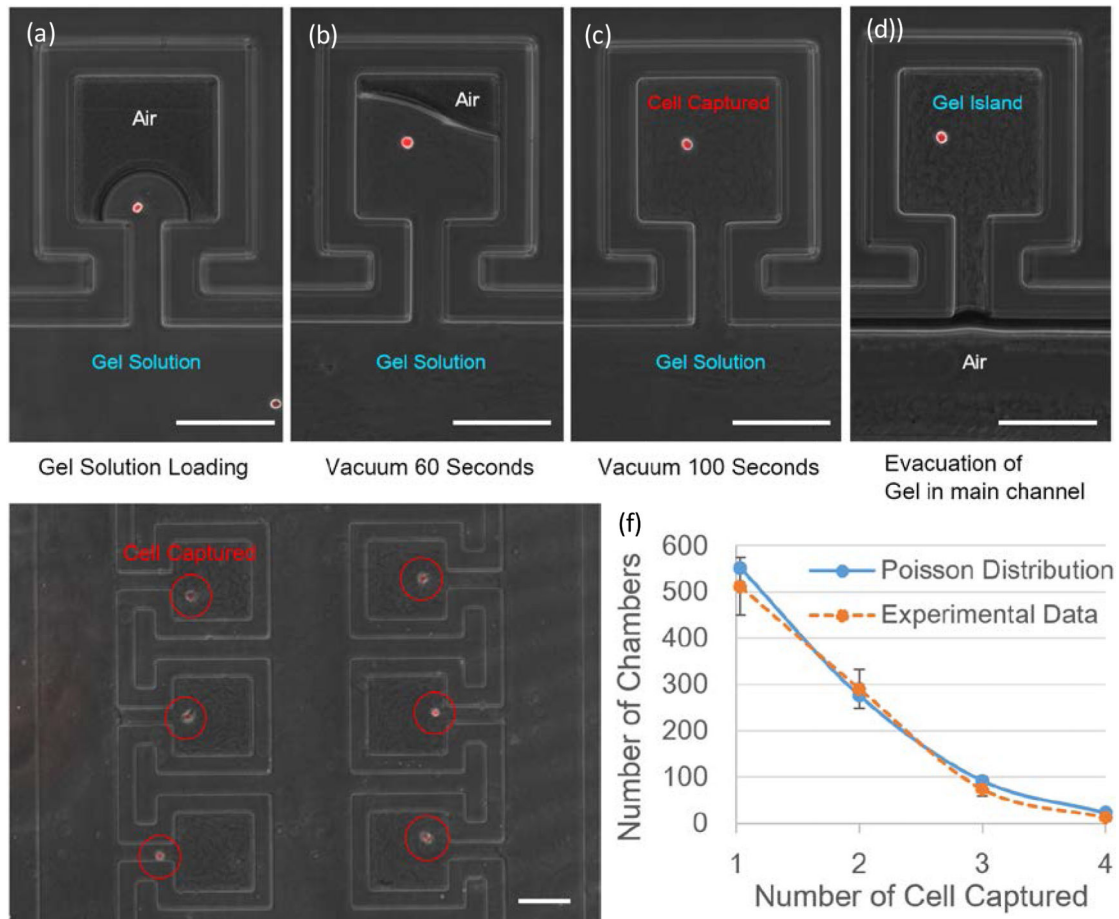
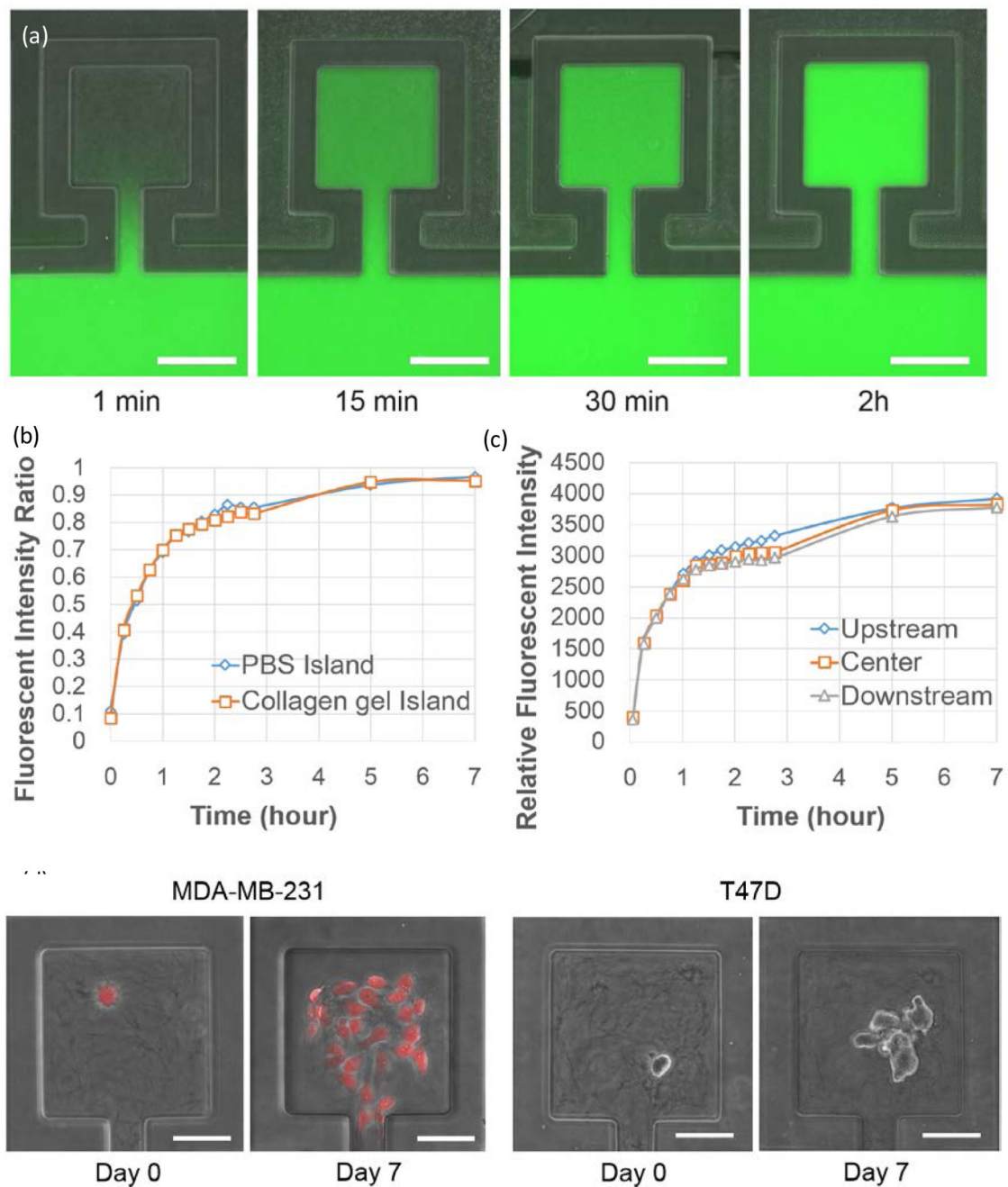


Figure.2.

(a) Loading the cell solution into the main channel. (b) Gel solution partially fills culture chamber after 60 seconds of applying vacuum. (c) Gel solution fully occupies the entire chamber after 100 seconds of applying vacuum, with a single cell captured. (d) The gel solution in the main channel is evacuated by pumping air. (e) Gel-island device loaded with MDA231 breast cancer cells. (f) Distribution of the number of captured cancer cells per chamber when loading 1500 cells into each device ($N = 3$). (Scale bar: 100 μm)

**Figure. 3.**

Long-term cell culture capability: (a) Device view of dextran conjugated fluorescein (Molecular weight = 40k) diffusion test at 1 minute, 15 minutes, 30 minutes and 2 hours. Fluorescein solution was loaded in the main channel and diffused in the collagen islands. (Scale bar: 100 μm) (b) Ratio of mean fluorescent intensity of chambers to mean fluorescent intensity of nearby main channel vs. time. (N = 5) (c) Relative fluorescent intensity in chambers at the upstream, center, and downstream of the device (N = 5). (d) On-chip cell culture of MDA-MB-231 and T47D breast cancer cells for 7 days. (Scale bar: 50 μm)

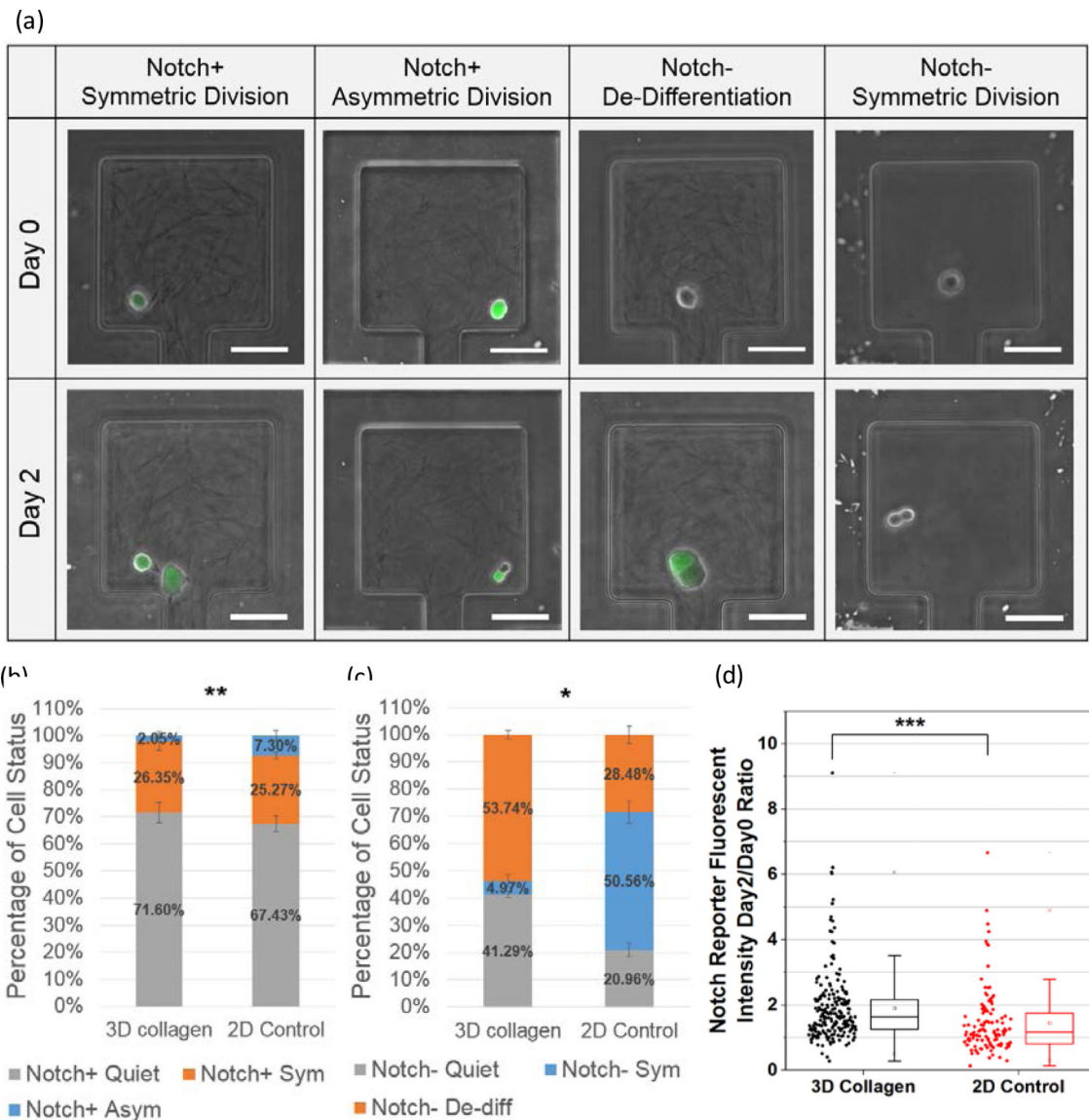
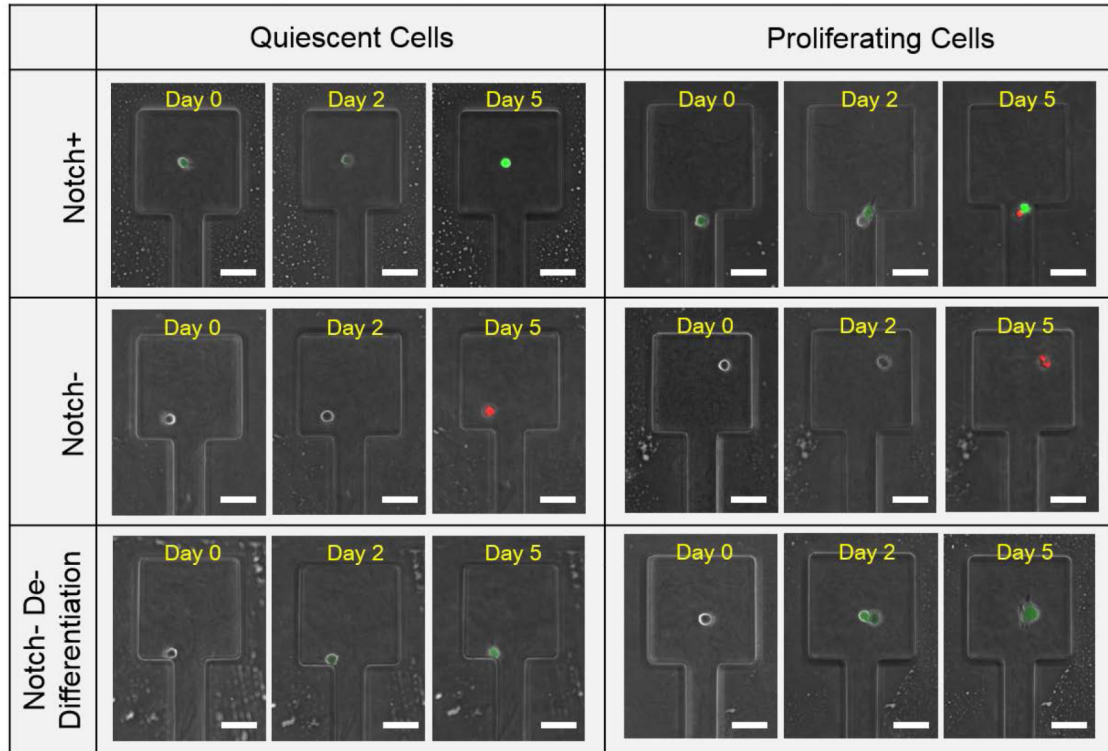


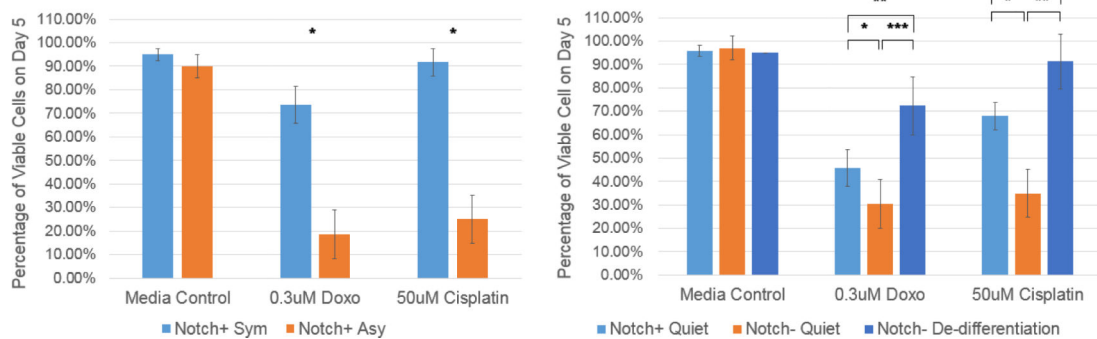
Figure 4.

T47D breast cancer cell differentiation: (a) Examples of different cell status after culturing on chip for 2 days. (b) T47D Notch+ cell status. (c) T47D Notch- cell status. The data samples used in the significance test of (b) and (c) are the ratio of Notch+ symmetric division population percentage to Notch+ asymmetric division population percentage in 3D collagen culture conditions vs. that in 2D Control culture conditions. (d) Distribution of Notch reporter gene fluorescent intensity ratio between 48 h (day 2) and 6 h (day 0) after cell loading under 2 culture conditions: 3D collagen gels (black, N = 209) and 2D culture media (red, N = 116). * Refers to $P < 0.05$, ** refers to $P < 0.01$, *** refers to $P < 0.001$, NS refers to not significant. (Scale bar: 50 μm)

(a)



(b)

**Figure 5.**

Drug susceptibility test of T47D Notch+ breast cancer cells under 2 mg/mL 3D collagen gel condition, cultured on chip for 48 hours followed by 72 hours drug treatment: (a) Examples of cell status, its drug response (the green fluorescence in the day 0 and day 2 images is from GFP, the green/red fluorescence in day 5 is from the Live/Dead dye). (b) Drug susceptibility comparison between symmetrically divided Notch+ cells (blue, N = 3) and asymmetrically divided Notch+ cells (orange, N = 3). (c) Drug susceptibility comparison between 3 types of non-proliferating cells: Notch+ quiescent cells (light blue, N = 3), Notch- quiescent cells (orange, N = 3), and Notch- de-differentiation cells (dark blue, N = 3). * Refers to $P < 0.05$, ** refers to $P < 0.01$, and *** refers to $P < 0.001$. (Scale bar: 50 μm)